Switchable Ultrastrong Coupling in Circuit QED

B. Peropadre,[1] P. Forn-Díaz,[2] E. Solano,[3,4] and J. J. García-Ripoll[1]

[1]*Instituto de Física Fundamental, CSIC, Serrano 113-bis, 28006 Madrid, Spain*
[2]*Quantum Transport Group, Kavli Institute of Nanoscience, Delft University of Technology, Lorentzweg 1, 2628 CJ Delft, The Netherlands*
[3]*Departamento de Química Física, Universidad del País Vasco—Euskal Herriko Unibertsitatea, Apartado 644, 48080 Bilbao, Spain*
[4]*IKERBASQUE, Basque Foundation for Science, Alameda Urquijo 36, 48011 Bilbao, Spain*

(Received 19 January 2010; published 6 July 2010)

We propose different designs of switchable coupling between a superconducting flux qubit and a microwave transmission line. They are based on two or more loops of Josephson junctions which are directly connected to a closed (cavity) or open transmission line. In both cases the circuit induces a coupling that can be modulated in strength, reaching the so-called ultrastrong coupling regime in which the coupling is comparable to the qubit and photon frequencies. Furthermore, we suggest a wide set of applications for the introduced architectures.

DOI: 10.1103/PhysRevLett.105.023601 PACS numbers: 42.50.−p, 03.67.Lx, 85.25.−j

Superconducting quantum circuits [1] possess ingredients for quantum information processing and for developing on-chip microwave quantum optics [2]. After the first manipulations of few-level superconducting systems (qubits) [3–5], the real boost came with the achievement of the strong coupling regime between qubits and confined microwave photons [6–8]. The initial qubit-cavity couplings of 10–100 MHz exceeded by orders of magnitude the rate at which photons leak out of the resonator, but the use of the transmon qubit [9] improved those numbers by a factor of 2–3 reaching a strength that is comparable only to the state of the art in microwave quantum optics [10,11]. More recently, proof-of-principle theoretical and experimental studies have paved the way to the ultrastrong coupling regime [12–14], where the coupling approaches the qubit transition frequency and the Jaynes-Cummings model of cavity QED [10,14] breaks down [15,16], and a door opens to the rather unexplored physics beyond the rotating-wave approximation [17,18].

The strong coupling regime in circuit QED has made possible an incredible variety of experiments, such as dispersive readouts of qubits [19], resolving the photon numbers in cavity [20], multiphoton excitations of the Jaynes-Cummings model [21], preparing nonclassical states of a resonator [22], full quantum tomography of the microwave radiation field [23], or the Tavis-Cummings model [24], etc. However, all those experiments have something in common: The microwave field is confined inside a resonator. In other words, the transmission line spectrum is discrete and the coupling between qubits and photons could be switched on and off by tuning the qubit [25] or cavity frequency [26]. While the switchability of the coupling has been proposed for open lines [27,28], this has not been achieved in the ultrastrong coupling regimes.

In this work, we will introduce a novel circuit QED design where the qubit is ultrastrongly coupled to a transmission line, open or not, with a coupling that can be tuned in strength and kind by applying an external flux bias. Our proposal uses the type of designs shown in Fig. 1, where the qubit is built in direct contact with the transmission line. It has been shown theoretically [14], and demonstrated experimentally [13], that the system admits an effective description based on a two-level system—the current in the loop—ultrastrongly coupled to the photons in the line. We will boost these ideas and show that, by means of induced quantum interference, one is capable of cancelling the ultrastrong coupling, effectively rotating the qubit basis, or activating higher-order nonlinearities. This fully controllable coupling tunability opens the path for new experimental results and nontrivial applications. A very important one is switching on and off the interaction in order to control the qubit evolution with subnanosecond resolution, allowing one to resolve the emission and propagation of single photons, measuring their light cone, and studying the propagation of entanglement between qubits coupled to the same transmission line [29]. Straightforward

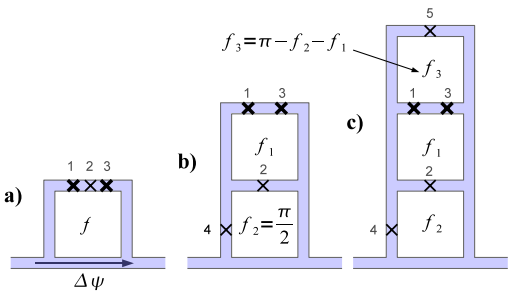

FIG. 1 (color online). Schemes for ultrastrong coupling between a qubit and a transmission line. (a) Basic setup of a qubit coupled directly to the line. $\Delta\psi$ is the phase difference between the nodes in which the qubit and line intersect. (b) With a second loop, the coupling can be modulated. (c) A slightly improved setup in which the qubit is better decoupled from the flux f_2.

extensions of this work will also allow the implementation of ultrafast quantum switches between cavities and remote qubits or the design of qutrits with tunable couplings.

The basic design of the switchable coupling can be understood by using a few rules that focus on the inductive terms of the Hamiltonian. More precisely, we will concentrate on the dominant contributions to the energy, which are given by the Josephson junctions as $V(\phi_n) = -E_{Jn}\cos(\phi_n)$. Here, E_{Jn} denotes the Josephson energy of the nth junction, and ϕ_n is the phase difference between both sides of the junction. These phases are by the Josephson relation proportional to the flux across the device, $\phi = \varphi/\varphi_0$ with the reduced flux quantum $\varphi_0 = \hbar/2e$. The next rule is that around close loops the total flux is quantized in a multiple of $h/2e$. This quantization imposes relations between the flux jumps on different junctions, reducing the complexity of the problem, $\sum_n \phi_n = f + 2\pi n$, but it also introduces a control parameter which is the externally applied magnetic flux inside the loop, $f\varphi_0$. Finally, we will include an additional flux difference $\Delta\psi$ along the segment that is shared with the transmission line [see Fig. 1(a)] and which is the source of the coupling.

With these rules, one can analyze the setup from Fig. 1(a) and impose the usual flux qubit configuration, with two equal junctions $E_{J1} = E_{J3} = E_J$, and a smaller one $E_{J2} = \alpha E_J (\alpha < 1)$, and the quantization $\phi_1 + \phi_2 + \phi_3 - \Delta\psi = f + 2\pi n$. The result is an effective Hamiltonian that, for $f = \pi$, reads

$$\begin{aligned} H_J &= -E_J\cos(\phi_1) - \alpha E_J\cos(\phi_2) - E_J\cos(\phi_3) \\ &= E_J[\alpha\cos(\phi_+) - 2\cos(\phi_-/2)\cos(\phi_+/2)] \\ &\quad + \alpha E_J\Delta\psi\sin(\phi_+) + O(\Delta\psi^2). \end{aligned} \tag{1}$$

Note how this model combines a flux qubit term [4], where the most important variable is the linear combination $\phi_+ = \phi_3 + \phi_1$, with a coupling between the qubit degrees of freedom and the transmission line. When we introduce the capacitive terms, the qubit can be diagonalized and the model becomes

$$H \sim \tfrac{1}{2}\Omega\sigma_z + \alpha E_J\Delta\psi\sigma_x. \tag{2}$$

It is noteworthy to mention that the qubit-line coupling can remain in the ultrastrong regime [14], because it is proportional to the Josephson energy αE_J. However, the coupling always has the form $\sigma_x\Delta\psi$, and there are no parameters to tune the interaction.

A more versatile design, shown in Fig. 1(b), separates the three qubit junctions and the transmission line by a loop. The new Josephson junction adds a contribution to the energy, which is of the form $E_{J4}\cos(\phi_4) = \alpha_4 E_J\cos(f_2 - \phi_2 - \Delta\psi)$, while keeping the flux qubit quantization independent of the transmission line flux, $\Delta\psi$. The result is now

$$\begin{aligned} H = E_J[&-\alpha\cos(f_1 - \phi_+) - 2\cos(\phi_-/2)\cos(\phi_+/2)] \\ &+ \alpha_4 E_J\cos(f_1 + f_2 - \Delta\psi + \phi_+), \end{aligned} \tag{3}$$

with two independently adjustable parameters f_1 and $f_1 + f_2$. A numerical evaluation of the Hamiltonian in the qubit basis reveals that for $f_2 = \pi$ the effective coupling

$$H \sim \frac{1}{2}\Omega\sigma_z + \alpha_4 E_J\Delta\psi\sum_{r=x,y,z} c_r^1(\alpha, \alpha_4, f_1)\sigma_r \tag{4}$$

is linear in the field and has a tunable orientation $c_r^1(\alpha, \alpha_4, f_1)$.

Moreover, since the coupling term is strictly independent of the qubit Hamiltonian, it now becomes possible to switch on and off the interaction. The simplest way is to replace the fourth junction E_{J4} with a SQUID, so that a control flux over this loop will allow us to dynamically tune the coupling strength α_4. By using this technique, the mutual influence between the qubit and the transmission line can be completely suppressed in times of about 0.1 ns, which is much faster than the qubit-resonator dynamics [30]. Remark that in the ultrastrong coupling regime the rotating-wave approximation cannot be made, and the physics of Rabi oscillations does not apply.

A different setup which we consider in this work is shown in Fig. 1(c). We now included two equal junctions $E_{J5} = E_{J4} = \alpha_4 E_J$, and we add a new loop above the qubit with a control flux f_3. Working at $f_3 = \pi - f_2 - f_1$ we cancel a contribution $\cos(f_1 + f_2 + \phi_+)$ that appears in Eq. (3) when we move away from $f_2 = \pi$. The effective Hamiltonian now reads

$$H = \frac{1}{2}\Omega\sigma_z + \alpha_4 E_J\sum_{n=1,2\ldots}\Delta\psi^n\sum_{r=x,y,z} c_r^n(\alpha, \alpha_4, f_1, f_2)\sigma_r. \tag{5}$$

With the two free parameters $\{f_1, f_2\}$ we can (i) switch on and off the interaction, (ii) change the orientation, and (iii) increase the relevance of higher-order couplings.

We have analyzed these setups numerically, confirming that the coupling is ultrastrong and can be arbitrarily tuned. In order to do so, we first completed the theoretical model to include the capacitive terms which appear in the junctions and the line itself. We then diagonalized the Hamiltonian of what we identify as the qubit degrees of freedom and verified that they can still be treated under a two-level approximation. Finally, we expanded the interaction between the qubit and the transmission line in powers of the flux $\Delta\psi$ and computed the matrix elements of the interaction in the qubit basis.

The main results are shown in Figs. 2 and 3, corresponding to setups in Fig. 1(b) and 1(c). In the first figure we have explored the simplest switchable setup for various configurations of the qubit α and of the externally applied flux f_1. It is important to remark that we have a very good qubit for values of α well above the 0.8 which is normally considered. Furthermore, when $f_1 = \pi$ for both $\alpha < 1$ and

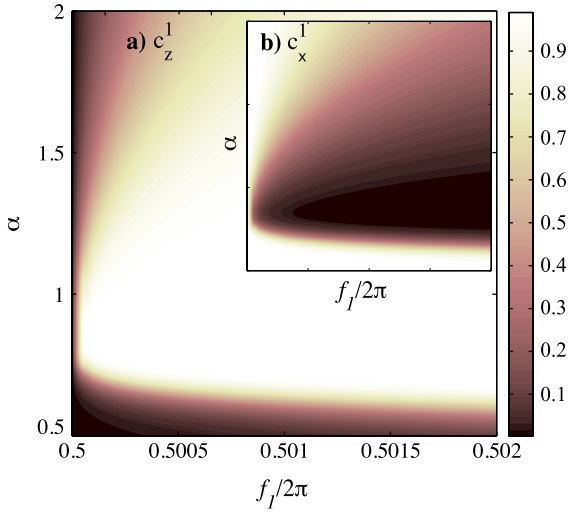

FIG. 2 (color online). For the Fig. 1(b) setup, coupling strengths as a function of the external flux f_1 and the qubit junction size $\alpha = E_{J2}/E_{J1}$, for $f_2 = \pi$. We plot (a) the normalized first-order coupling along the Z direction, $c_z^1 \sigma_z \Delta\psi$, and (b) across the XY plane.

$\alpha > 1$, the ground states are superpositions of left- and right-moving currents, and the interaction is proportional to σ_x, transversely to the qubit basis. When we apply a small flux difference increasing or decreasing f_1, we unbalance the populations of the two current states, the ground state acquires an effective magnetic dipole, and the interaction rotates from σ_z to $\sigma_{x,y}$.

The second set of plots is shown in Fig. 3 and corresponds to the three-loops setup [Fig. 1(c)]. We have chosen $\alpha = 2$ because it allows for a finer control in the rotation of the interaction σ_x to σ_z, but it is not essential. The tunability of the qubit manifests as follows: When f_1 is increased, the strength of $c_x^{1,2}$ decreases, causing an increase of $c_z^{1,2}$, much like in Fig. 2. But in addition to this, we now have complete freedom to change the value of f_2. Changes in this second flux result in a simultaneous deactivation of all couplings $c_{x,y,z}$, which become zero as seen in the dark horizontal stripes for $f_2 = (2n+1)\pi/2$ in Fig. 3(a) and in the zeros of c_x in Fig. 3(b). The switching capability, measured as $\min c_x/c_z$, is rather strong, 6×10^{-4} in this example, and improves by increasing α.

We may now address the absolute strength of the qubit-line coupling. For clarity, we will restrict to the case in which the line forms a single-mode resonator, which admits a trivial generalization to the continuum by summing over modes. The phase slip then becomes approximately [14]

$$\Delta\psi = \frac{\partial_x u(x)\Delta x}{\varphi_0}\sqrt{\frac{\hbar}{\omega C}}(a + a^\dagger) = \frac{2\pi\partial_x \Psi(x)\Delta x}{\Phi_0}(a + a^\dagger).$$

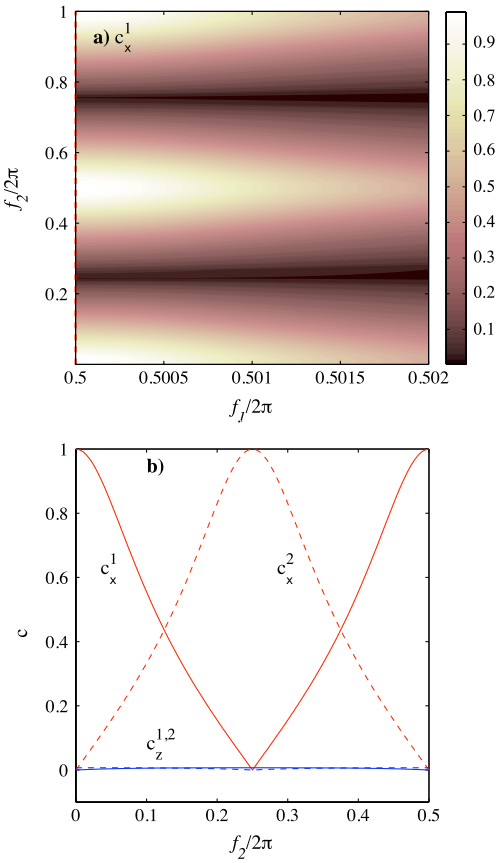

FIG. 3 (color online). (a) Following Eq. (5), normalized transverse coupling c_x^1 as a function of external fluxes f_1 and f_2 for the setup in Fig. 1(c), using $\alpha = 2.0$ and $\alpha_4 = 0.1$. (b) Cut at $f_1 = 0.5$ shows first-order (solid line) and second-order couplings (dashed line) of longitudinal (c_z, blue line) and transverse (c_x, red line).

Here $u(x)$ is the photon mode eigenfunction in the cavity, Δx is the separation between the two qubit-line intersections, ω is the cavity mode frequency, and C the resonator total capacitance. The dependence is thus similar to previous works meaning that we can achieve comparable ultrastrong couplings. Assuming a flux gradient $|\partial_x \Psi| = 65 \times 10^{-6}\Phi_0/\mu\text{m}$ and a qubit size $\Delta x = 5\ \mu\text{m}$, we reach a coupling $g = 2 \times 10^{-3} E_J$, which for a typical junction with $E_J = 250$ GHz implies a very strong 500 MHz coupling. The previous numbers are, however, pessimistic. An aluminum thin film penetration depth $\lambda_L = 150$ nm allows a larger flux gradient, of $1.7 \times 10^{-3}\Phi_0/\mu\text{m}$ or 25 times the previous coupling strength, that is up to 10 GHz. Either with these values, or by enhancing the phase slip with the use of an auxiliary junction [14], the fact is one can take the coupling strength deep in the ultrastrong regime with an interesting consequence, namely, the possibility of inducing nonlinearities in the transmission line [Fig. 3]. In the crudest approximation, the second-order coupling strength is proportional to $\alpha_4 E_J (2\pi\Delta x \partial_x \psi/\Phi_0)^2$. For a phase slip

of 0.01–0.03, that means a coupling $E_J \times (10^{-4}$–$10^{-3})$, or 25 to 250 MHz, according to the values mentioned before.

Throughout this work we neglected the coupling between the qubit and photons induced by the capacitive energy of the junctions, that is, terms of the form

$$H_{\mathrm{cap}} = \frac{\alpha_4}{1 + 2\alpha + 4\alpha_4} 2\pi\hbar\omega \frac{\partial_x \psi}{\Phi_0} \Delta x i(a - a^\dagger) q_+, \quad (6)$$

where $q_+ = (-i\partial/\partial\phi_+)$ is the conjugate operator to the flux qubit variable ϕ_+. This term, and a similar one for E_{J5} [Fig. 1(c)], gives a negligible coupling strength $\sim 10^{-3}\hbar\omega$.

We envision several applications of the switchable coupling introduced before. The first one would be to perform quantum gates between arbitrary qubit pairs of a row coupled to a transmission line. By decoupling all qubits except those chosen to perform a two-qubit gate, it should be possible to perform operations as the swap of quantum information between the qubit and the line modes or between both qubits. This scheme has an important advantage, namely, that the qubit switching happens for precise flux values, depending only on geometric properties and not on the precise eigenenergies or fabricated junction properties. A second application would be decoupling a qubit from the transmission line and coupling it to slower measurement devices, especially after having performed an ultrastrong coupling evolution [31]. Furthermore, since the coupling may be switched on and off in about 0.1 ns, this enhanced resolution can also be used for the measurement of quantum microwaves. More precisely, given that one qubit may act as a perfect mirror for individual photons, a combination of one or more may be used as streak camera for stroboscopic measurements of wave packets. A fourth application is the deterministic generation of propagating single- and two-photon pulses. This would work by decoupling the qubit, exciting it, and then activating an ultrastrong coupling dynamics. The qubit would decay in a few nanoseconds, emitting either a single photon (linear coupling) or two of them (nonlinear one) in a wave packet whose shape can be tailored with a second qubit.

In conclusion, we believe that the future access to the physics of switchable ultrastrong coupling will pave the way to novel and otherwise inaccessible physics, including key applications to quantum microwave technologies.

P. F.-D. acknowledges support from NanoNed. E. S. acknowledges funding from UPV-EHU Grant No. GIU07/40, Spanish MEC Project No. FIS2009-12773-C02-01, EuroSQIP, and SOLID European projects. J. J. G.-R. and B. P. thank funding from Spanish Projects No. MEC FIS2006-04885 and No. CSIC 200850I044 and the CSIC JAE-PREDOC2009 grant.

[1] J. Clarke and F. K. Wilhelm, Nature (London) **453**, 1031 (2008).
[2] R. J. Schoelkopf and S. M. Girvin, Nature (London) **451**, 664 (2008).
[3] V. Bouchiat, D. Vion, P. Joyez, D. Esteve, and M. H. Devoret, Phys. Scr. **T76**, 165 (1998).
[4] J. E. Mooij *et al.*, Science **285**, 1036 (1999).
[5] J. M. Martinis, M. H. Devoret, and J. Clarke, Phys. Rev. Lett. **55**, 1543 (1985).
[6] A. Blais, R.-S. Huang, A. Wallraff, S. M. Girvin, and R. J. Schoelkopf, Phys. Rev. A **69**, 062320 (2004).
[7] A. Wallraff *et al.*, Nature (London) **431**, 162 (2004).
[8] I. Chiorescu *et al.*, Nature (London) **431**, 159 (2004).
[9] J. Koch *et al.*, Phys. Rev. A **76**, 042319 (2007).
[10] S. Haroche and J.-M. Raymond, *Exploring the Quantum* (Oxford University Press, New York, 2006).
[11] M. Brune *et al.*, Phys. Rev. Lett. **101**, 240402 (2008).
[12] M. Devoret, S. Girvin, and R. Schoelkopf, Ann. Phys. (N.Y.) **16**, 767 (2007).
[13] A. A. Abdumalikov, O. Astafiev, Y. Nakamura, Y. A. Pashkin, and J. Tsai, Phys. Rev. B **78**, 180502 (2008).
[14] J. Bourassa *et al.*, Phys. Rev. A **80**, 032109 (2009).
[15] C. Ciuti, G. Bastard, and I. Carusotto, Phys. Rev. B **72**, 115303 (2005).
[16] G. Günter *et al.*, Nature (London) **458**, 178 (2009).
[17] F. De Zela, E. Solano, and A. Gago, Opt. Commun. **142**, 106 (1997).
[18] A. P. Hines, C. M. Dawson, R. H. McKenzie, and G. J. Milburn, Phys. Rev. A **70**, 022303 (2004).
[19] S. Filipp *et al.*, Phys. Rev. Lett. **102**, 200402 (2009).
[20] D. I. Schuster *et al.*, Nature (London) **445**, 515 (2007).
[21] F. Deppe *et al.*, Nature Phys. **4**, 686 (2008).
[22] M. Hofheinz *et al.*, Nature (London) **454**, 310 (2008).
[23] M. Hofheinz *et al.*, Nature (London) **459**, 546 (2009).
[24] J. M. Fink *et al.*, Phys. Rev. Lett. **103**, 083601 (2009).
[25] M. Mariantoni *et al.*, Phys. Rev. B **78**, 104508 (2008).
[26] J. R. Johansson, G. Johansson, C. M. Wilson, and F. Nori, Phys. Rev. Lett. **103**, 147003 (2009).
[27] Y.-D. Wang, A. Kemp, and K. Semba, Phys. Rev. B **79**, 024502 (2009).
[28] A. J. Kerman and W. D. Oliver, Phys. Rev. Lett. **101**, 070501 (2008).
[29] C. Sabín, J. J. García-Ripoll, E. Solano, and J. León, Phys. Rev. B **81**, 184501 (2010).
[30] C. M. Wilson (private communication).
[31] I. Lizuain, J. Casanova, J. J. García-Ripoll, J. G. Muga, and E. Solano, Phys. Rev. B (to be published).